A physical interpretation of the collinear reactive scattering resonances in the F+HD, H_2, and D_2 systems

Vasil K. Babamov[a] and Aron Kuppermann

Arthur Amos Noyes Laboratory of Chemical Physics, California Institute of Technology, Pasadena, California 91125[b]

(Received 2 June 1981; accepted 24 August 1981)

A simple model is presented that explains the main characteristics of the low energy resonances found in accurate quantum mechanical scattering calculations of collinear reactive collisions of the type F + XY→FX + Y, where X and Y are H or D atoms. The wave function of the resonance complex can be approximately described by a product of a function of the F–XY distance and a vibrationally adiabatic function of the X–Y distance. The corresponding vibrational eigenvalues of the XY diatom as a function of the F–XY distance form an attractive, effective one-dimensional potential for the F–XY motion that supports a quasibound state. The resulting resonance is broadened by its interaction with the reagent and product scattering states. The resonance energies given by the model are in good agreement with those obtained by exact scattering calculations for the F + HD, H_2, and D_2 systems.

I. INTRODUCTION

There has been a considerable effort in recent years directed toward the understanding of the dynamics of the $F + H_2$ reaction.[1,2] Besides being important technologically for the design of chemical lasers, this reaction is one of the simplest examples of a highly exothermic chemical reaction with a low activation barrier and can be regarded as the prototype model for understanding the dynamics of such reactions. The relatively small number of electrons in the $F + H_2$ system facilitates the calculation of the *ab initio* potential surfaces for the nuclear motion. In recent years, several extensive calculations of this type for the ground electronic state potential energy surface have been performed[3-5] which determine the surface to within less than 1 kcal/mol. Further refinements to ~0.1 kcal/mol, an accuracy already attained for the $H + H_2$ reaction in the regions of the surface most important for the dynamics,[6,7] can be expected with the advancement in the *ab initio* techniques in the next few years.

The dynamics of the $F + H_2$ reaction, and of the isotopic variations in which one or both of the H atoms are replaced by D atoms, have been studied extensively using classical trajectories for both the collinear and the three-dimensional cases.[8-18] The results have been used to develop semiempirical potential energy surfaces for which the dynamical studies give rate constants in good agreement with the experimental ones.[2,8,10,16] Most such semiempirical surfaces are in good qualitative agreement with the *ab initio* ones, which gives some confidence in the correctness of the main features of the surface.

Several collinear quantum mechanical scattering calculations have been performed using semiempirical potential energy surfaces for $F + H_2$ and its isotopic variations[18-23] as well as an analytic fit to an *ab initio* surface.[21] The comparison of the quantum with the classical and the semiclassical results[18] revealed the existence and gave some indication of the importance of various quantum effects. The large exothermicity of the reaction and the number of accessible quantum states of the products due to it makes accurate three-dimensional (3*D*) coupled-channel calculations, and the possibility of direct comparison of theory and experiment, difficult at the present time. However, approximate 3*D* calculations of the integral state-to-state cross sections of $F + H_2$[24] and of the relative vibrational product distributions[25] have been performed, which gives some insight into the 3*D* dynamics of the system.

Crossed molecular beam studies of the detailed dynamics of the $F + D_2$[26] and $F + H_2$[27] reactions have also been performed. For both reactions, vibrationally resolved angular distributions of the products have been obtained which provide detailed data for testing theoretical models.

A number of accurate collinear quantum mechanical scattering calculations on the $F + H_2$ reactions and its isotopic variations[18-23] on different potential energy surfaces have shown the existence of narrow peaks in the state-to-state or total reactive transition probability vs energy curves. These peaks are accompanied by rapid changes in the phases of the scattering matrix as a function of the energy as well as in its eigenphases.[28] A recent collision lifetime matrix analysis of accurate coupled-channel calculations, performed in our laboratory, has shown that one single eigenvalue of that lifetime matrix, when plotted as a function of energy, displays a pronounced positive maximum.[29] These features have been interpreted[18-21,28,29] as resonance effects due to the formation of a long-lived, almost bound triatomic complex. Closely related behavior can be found[24] in the approximate 3*D*-partial wave results for the $F + H_2$ reaction on the Muckerman V LEPS surface, indicating that the formation of a long-lived collinear or nearly collinear triatomic complex is likely to play an important role in the reaction 3*D* collision dynamics of this system. Exact partial wave calculations have suggested that the formation of a collinear complex plays an important role in the $H + H_2$ 3*D* collision dynamics.[30] No accurate 3*D* calculations of the differential state-to-state cross sections for the $F + H_2$ or any other reaction in the energy region in which resonances can be formed

[a]Present address: Centro de Graduados, Instituto Technologico de Tijuana, Apdo. Postal 1166, Tijuana, B.C., Mexico.
[b]Contribution No. 6441.

 0021-9606/82/161891-13$02.10

have been reported, and it is not known how the details of the angular distribution are affected by the existence and the characteristics of the long-lived complex. The results of the crossed molecular beam experiments for $F + D_2$[26] and $F + H_2$[27] show a broadening of the angular distribution at energies at which the formation of a long-lived complex can be expected. An angular distribution of the reaction products symmetric around a center-of-mass scattering angle of 90° is a consequence of the existence of a quasibound state that exists for a full rotation of the complex or longer.[31] More conclusive evidence of the existence of a complex, especially a shorter-lived one, and more importantly, information about the nature of the interatomic forces that cause it, can be obtained by learning more about the correlation between the resonance characteristics and the resulting observable experimental quantities, especially the collisional energy dependence of the reaction products angular distributions.

The long-lived complexes responsible for the resonance phenomena obtained from quantum mechanical calculations are normally located in the strong interaction region of the potential energy surface in which all three atoms are close to each other. Consequently, the characteristics of the resonance features are determined mainly by the structure of the potential energy surface in that region of configuration space, and therefore, are capable of providing information about its details. Study of the dynamics of these complexes and of their correlation with the features of the potential energy surface in the strong interaction region and with their experimental manifestation can provide a tool for the experimental determination of interatomic forces at small interatomic distances in systems that form resonant states.

Understanding the nature of a long-lived complex in a collinear collision and developing simple models that are capable of simulating its main dynamical features and of approximating its energy and lifetime is the first step in establishing such a correlation. Since accurate solutions of the Schrödinger equation for a reactive system at energies at which resonances occur are available for collinear collisions, the validity of approximate models can be directly tested for a collinearly restricted complex. An extension to a noncollinearly restricted model for collinearly dominated potential energy surfaces, which seems to describe both the $H + H_2$ and $F + H_2$ reactions, can further be developed.

The dynamics of the formation of quasibound states in a collinear atom–diatomic molecule collision is somewhat simpler in the case when no reaction can occur, i.e., for inelastic collisions. Resonances in collinear inelastic collisions have been studied on both simplified models[32,33] and realistic potential energy surfaces,[34,35] and highly accurate simple approximate models have been developed for such nonreactive systems.[32–35] The long-lived complex has two degrees of freedom and, for the systems for which good approximate models have been developed, its dynamics can be described by that of a two-dimensional oscillator with two weakly coupled modes. One of the modes can be closely approximated by the vibration of the isolated diatomic molecule that participates in the collision.

The dynamics of a reactive collinear system are somewhat more complex. There are two different kinds of diatomic molecule vibrations, those of the reactant and those of the product molecule, and they appear to be strongly mixed in the strong interaction region of the potential energy surface. The quantum mechanical approximate models used for studying resonances in collinear reactive collisions are usually based on some kind of coordinates that transform smoothly from those appropriate for reactants to those appropriate for products.[20,36–38]

Significant progress has also been attained in developing semiclassical procedures for locating and describing the dynamics of resonances in both inelastic[33,39] and reactive collisions.[40]

The model used for describing the resonances in inelastic scattering,[35] in which one of the modes of the quasibound complex is assumed to be equivalent to the asymptotic vibration of the colliding molecule, has been used to explain the resonances in the $I + H_2$ system on an approximate (LEPS) potential energy surface.[41] A significant feature of this surface is that it has wells in both reactant and product channel regions well separated from each other. The dynamics of the quasibound complexes in those wells is similar to the dynamics of the reactants and of the products, and the model has given excellent approximations for the resonance energies. However, these wells are probably due to an artifact of the LEPS functional form used and are nonphysical.

It was found that resonance peaks in the collinear $F + H_2$ system appear in the vicinity of and are closely related to the opening of vibrational channels.[18] The resonance features are strongly influenced by the details of the potential energy surface; slightly different surfaces lead to completely different resonance structures.[21] Recently, a detailed analysis of the reaction dynamics in terms of curvilinear coordinates that smoothly change from reactants to products[20] showed that no single-channel model in those coordinates can provide a satisfactory explanation for the nature of the resonance.

The proposed surfaces for the $F + H_2$ reaction do not have wells in the reactant or product regions, and since the barrier at the saddle point is low, there appears to be a smooth passage for the system to go from reactants to products, making it possible for the asymptotic reactant and product vibration to blend into each other in the interaction region and to lose their distinction. The appreciable reactive transition probabilities for most of the isotopic variations of $F + H_2$ reinforce such an interpretation.

On the other hand, the numerical results[18c] for the collinear $F + HD \rightarrow FH + D$ reaction on the Muckerman V potential energy surface show a narrow resonance peak in the middle of a wide energy range on which the scattering is almost purely elastic. The obvious conclusion is that despite the smooth shape of the surface

there is not much mixing between the reactant and the product states during the collision in this energy range and that the vibrational states of the reactants and the products, although probably subject to some distortion, retain their distinction and character throughout the collision. One of the distorted vibrational states of the reactants or of the products, is, hence, likely to be a distinct mode of the motion of the quasibound complex that is responsible for the resonance.

A comparison among the numerical reaction probability results for the F + HD, F + H_2, and F + D_2 systems reveals some common features in the corresponding low energy resonance peaks and indicates that a similar mechanism is likely to be responsible for the lowest energy resonances in all three systems. In this paper, a model of this low-energy resonance based on the adiabaticity of the ground vibrational state of the reactants during a collision between the reactants is developed and tested against accurate coupled-channel calculations on the Muckerman V LEPS potential energy surface, which has no wells. The main reason for this choice is that accurate collinear quantum mechanical collision probability results for four isotopic variations of the reaction are available for this surface.[18]

The details of the approach and its mathematical formulation are given in Sec. II. The model for the lowest energy resonance, the results obtained from it, and their comparison with accurate coupled-channel calculations are given in Sec. III. The consequences of the model and their relevance for the study of the actual F + H_2 $3D$ reaction dynamics are discussed in Sec. IV. In Sec. V, we summarize the results and conclusions.

II. MATHEMATICAL MODEL

The Schrödinger equation for the collinear A + BC → AB + C reaction along the BC axis can be written in terms of the Jacobian coordinates for the reactants or products as

$$\left[-\frac{\hbar^2}{2M_\lambda}\frac{\partial^2}{\partial R_\lambda'^2}-\frac{\hbar^2}{2m_\lambda}\frac{\partial^2}{\partial r_\lambda'^2}+V(r_\lambda', R_\lambda')\right]\psi(R_\lambda', r_\lambda') = E\psi(R_\lambda', r_\lambda'), \quad (\lambda=\alpha,\gamma), \tag{2.1}$$

where r_α' is the BC distance, R_α' is the distance of A to the center of mass of BC, m_α is the reduced mass of the BC pair, M_α is the reduced mass for the motion between A and BC, V is the potential energy function for the system, and ψ its energy eigenfunction. The same symbols with subscript γ denote the corresponding quantities for the reverse reaction. In Delves scaled coordinates[42]

$$R_\lambda = a_\lambda R_\lambda', \quad r_\lambda = a_\lambda^{-1} r_\lambda', \quad a_\lambda = (M_\lambda/m_\lambda)^{1/4}, \tag{2.2}$$

Eq. (2.1) becomes

$$\left[-\frac{\hbar^2}{2\mu}\left(\frac{\partial^2}{\partial R_\lambda^2}+\frac{\partial^2}{\partial r_\lambda^2}\right)+V(r_\lambda, R_\lambda)\right]\psi(R_\lambda, r_\lambda) = E\psi(R_\lambda r_\lambda), \tag{2.3}$$

where

$$\mu = \left(\frac{m_A m_B m_C}{m_A+m_B+m_C}\right)^{1/2}$$

is an effective reduced mass for the system, m_X being the mass of atom X (= A, B, C).

At large R_λ, the potential $V(r_\lambda, R_\lambda)$ in Eq. (2.3) does not depend on R_λ in the λ arrangement channel region of configuration space, and the solutions of that equation in that region are of the form

$$\bar{\psi}(R_\lambda, r_\lambda) = \bar{g}_i^\lambda(R_\lambda)\bar{\phi}_i^\lambda(r_\lambda), \tag{2.4}$$

where $\bar{\phi}_i^\lambda(r_\lambda)$ is the ith vibrational wave function for the unperturbed molecule AB or BC, i.e., the solution of

$$\left[-\frac{\hbar^2}{2\mu}\frac{d^2}{dr_\lambda^2}+V(r_{\lambda,\infty})\right]\bar{\phi}_i^\lambda(r_\lambda) = \bar{\epsilon}_i^\lambda\bar{\phi}_i^\lambda(r_\lambda), \tag{2.5}$$

and $\bar{g}_i^\lambda(R_\lambda)$ is the free particle wave function for the motion of the center of mass of BC relative to A or AB relative to C,

$$\bar{g}_i^\lambda(R_\lambda) = \exp(\pm ik_i^\lambda R_\lambda); \quad k_i^\lambda = \frac{1}{\hbar}[2\mu(E-\bar{\epsilon}_i^\lambda)]^{1/2}. \tag{2.6}$$

In Eqs. (2.5) and (2.6), $\bar{\epsilon}_i^\lambda$ is the vibrational energy of the isolated diatomic molecule AB or BC.

For smaller values of R_λ, the vibrational eigenfunctions of the diatomic molecule are perturbed by the presence of the third atom at a distance R_λ. The perturbed wave function $\phi_i^\lambda(r_\lambda; R_\lambda)$ can be obtained by solving Eq. (2.3) at a fixed value of R_λ,

$$\left[-\frac{\hbar^2}{2\mu}\frac{d^2}{dr_\lambda^2}+V(r_\lambda, R_\lambda)\right]\phi_i^\lambda(r_\lambda;R_\lambda) = \epsilon_i^\lambda(R_\lambda)\phi_i^\lambda(r_\lambda;R_\lambda) \quad (\lambda=\alpha,\gamma), \tag{2.7}$$

with the boundary conditions

$$\phi_i^\lambda(0;R_\lambda) = \phi_i^\lambda(r_{\lambda_{max}};R_\lambda) = 0, \tag{2.8}$$

where $r_{\lambda_{max}}$ is the value of r_λ that corresponds to the configuration in which B coincides with A (for $\lambda=\alpha$) or C (for $\lambda=\gamma$). These eigenfunctions ϕ_i^λ form a complete set of real orthogonal functions in the r_λ space.

At low collision energies, the vibrational motion of BC (or AB) along r_λ in the R_λ, r_λ configuration space may be much faster than the relative motion of A and BC (or AB and C) along R_λ, and an effective adiabatic separation of those two modes of motion can be expected.[37,43-46] In such cases, one can approximate the solution of Eq. (2.3) at any R_λ by an expression that reduces to Eq. (2.4) at large R_λ, namely,

$$\psi(r_\lambda, R_\lambda) \cong g_i^\lambda(R_\lambda)\phi_i^\lambda(r_\lambda;R_\lambda), \tag{2.9}$$

where $g_i^\lambda(R_\lambda)$ is the wave function for the motion along R_λ on the effective potential determined by the $\epsilon_i^\lambda(R_\lambda)$ of Eq. (2.7).

In the regions in which the potential is nearly separable in terms of R_λ and r_λ, such as the reactant (or the product) valley of the potential (see Fig. 1) outside the interaction region, Eq. (2.9) will obviously be valid. In the strong interaction region where the potential is not nearly separable, Eq. (2.9) will be valid only if there is a good separation of the velocities along r_λ and R_λ, and if none of the $\lambda' \neq \lambda$ states $\phi_i^{\lambda'}(r_\lambda; R_{\lambda'})$ is nearly degenerate with the λ state $\phi_i^\lambda(r_\lambda; R_\lambda)$ that appears in that equation. The separation of velocities condition is usually satisfied if M_λ/m_λ is much larger than unity.

The nature of the approximations used in assuming Eq. (2.9) can be examined more systematically by using

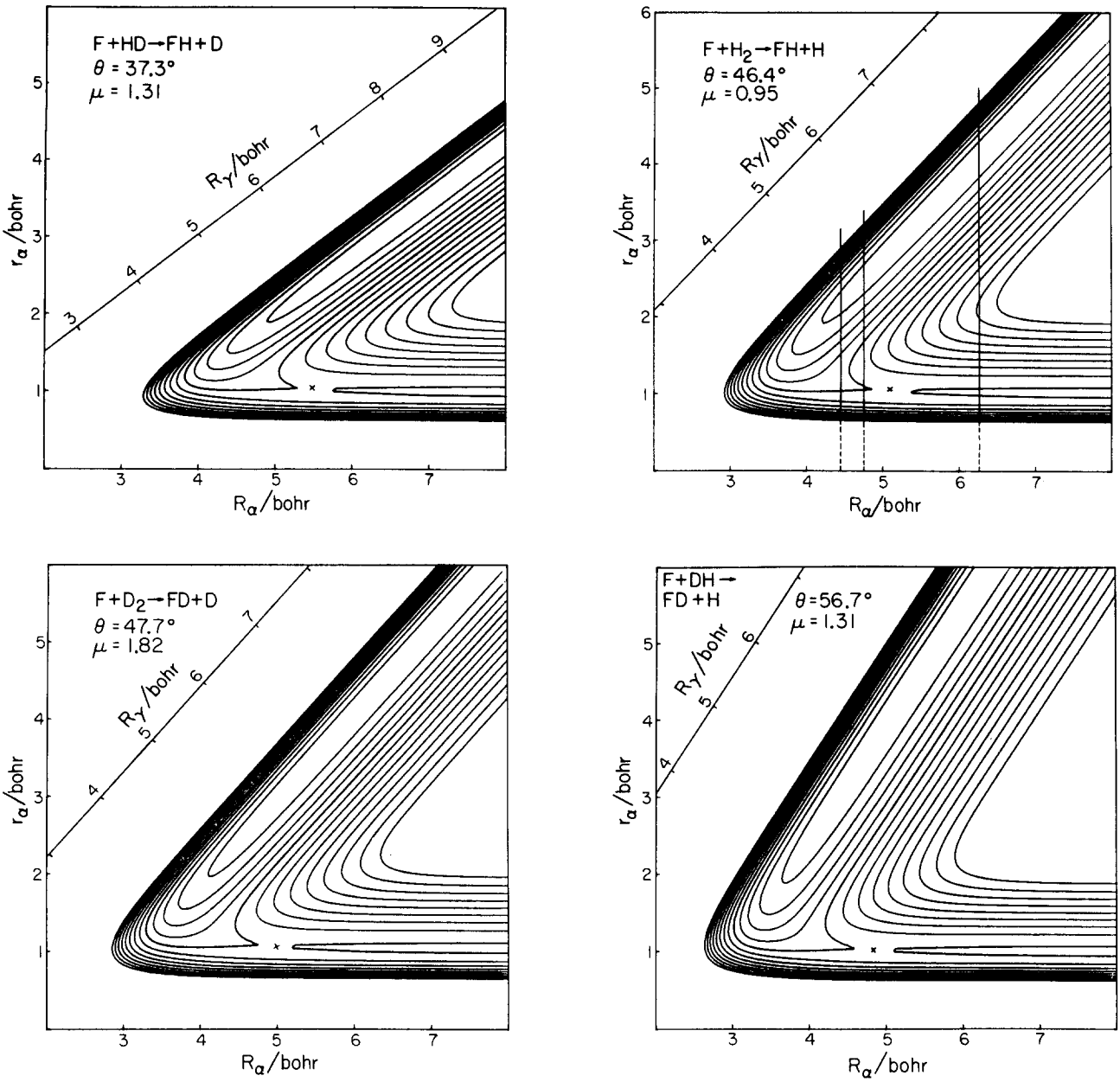

FIG. 1. Contour plot of the Muckerman V potential energy surface for the F + HD, F + H_2, F + D_2, and F + DH systems in the Delves scaled coordinates R_α, r_α. θ represents the skew angle between the R_γ and R_α axes and μ the effective mass of Eq. (2.3) in units of the H atom mass. The zero of energy is the bottom of the isolated hydrogenic molecule well. The energies of the contours are from −1.154 to 2.446 eV, uniformly spaced by 0.3 eV. The x mark indicates the position of the saddle point. The vertical lines on the F + H_2 plot denote the cuts for which the profile of the surface is shown on Fig. 2.

the ϕ_i^λ from Eq. (2.7) as a basis set for expanding the solution of Eq. (2.3)

$$\psi(r_\lambda, R_\lambda)=\sum_j g_j^\lambda(R_\lambda)\phi_j^\lambda(r_\lambda; R_\lambda)\,. \tag{2.10}$$

Substituting Eq. (2.10) in Eq. (2.3), premultiplying by $\phi_i^{\lambda*}(r_\lambda; R_\lambda)$ and integrating over r_λ, one gets a set of coupled ordinary differential equations for the coefficient wave functions $g_i^\lambda(R_\lambda)$

$$-\frac{\hbar^2}{2\mu}\frac{d^2g_i^\lambda}{dR_\lambda^2}-\frac{\hbar^2}{2\mu}\sum_j\left[2\langle\phi_i^\lambda|\frac{d}{dR_\lambda}|\phi_j^\lambda\rangle\frac{d}{dR_\lambda}+\langle\phi_i^\lambda|\frac{d^2}{dR_\lambda^2}|\phi_j^\lambda\rangle\right]$$

$$\times g_j^\lambda=(E-\epsilon_i^\lambda)g_i^\lambda \quad i=0,1,2,\ldots\,. \tag{2.11}$$

Equations (2.11) constitute an infinite set of coupled ordinary differential equations fully equivalent to Eq. (2.3). By solving them[47] and imposing the correct scattering boundary conditions, one can, in principle, obtain the full scattering solution of Eq. (2.3).

More importantly, however, Eq. (2.11) can be used as a starting point for developing simple approximations. If the elements that couple the state i with all the others are small in or near the R_λ region of classical motion in state i [i.e., where $\epsilon_i^\lambda(R_\lambda)\leq E$], the $g_i^\lambda(R_\lambda)$ can be viewed as a weakly perturbed solution of, and successfully approximated by, the solution of the equation

$$-\frac{\hbar^2}{2\mu}\frac{d^2g_i^\lambda(R_\lambda)}{dR_\lambda^2}+\epsilon_i^\lambda(R_\lambda)g_i^\lambda(R_\lambda)=Eg_i^\lambda(R_\lambda) \qquad (2.12)$$

obtained from Eq. (2.11) by neglecting the coupling terms.

The potential energy function $V(r_\lambda, R_\lambda)$ which through Eq. (2.7) generates the effective potential $\epsilon_i^\lambda(R_\lambda)$ in Eqs. (2.11) and (2.12) is, for large values of R_λ, a double minimum potential. For $\lambda=\alpha$ (see Fig. 2 with $R_\alpha=6.27$ bohr, for example), the well at the left resembles the vibrational potential of the isolated diatomic reactant molecule BC and becomes equivalent to it as $R_\alpha\to\infty$. The well at the right represents the products region of the potential energy surface; the coordinate r_α is, however, not appropriate for the product vibration (which is described by $\lambda=\gamma$) so that the motion in that part of the potential along r_α is not equivalent to that vibration. Only the solutions that are localized in the left well of the potential $V(r_\alpha, R_\alpha)$ evolve adiabatically from a particular vibrational state of the reactants and have the physical meaning of quasistationary vibrational states of the BC molecule perturbed by the presence of the atom A. The remaining solutions, localized in the right well of the double-well potential [Fig. 2(c)], do not correspond to stationary states of the products at large R_α and are included in Eq. (2.10) only for the purpose of making the basis set given by Eq. (2.7) complete and hence, making Eq. (2.11) rigorously equivalent to the Schrödinger equation.

The effective adiabatic potential $\epsilon_i^\lambda(R_\lambda)$ for the motion along R_λ in Eq. (2.12) determined by the eigenvalues of the perturbed vibrational Hamiltonian in Eq. (2.7) can have a minimum at a finite value of R_λ (see Fig. 3). As a result, the eigenvalues $\epsilon_i^\lambda(R_\lambda)$, which appear in Eq. (2.12), will either support bound states or exhibit resonances at some energies. If the coupling of $g_i^\lambda(R_\lambda)$ to the other states in Eq. (2.11) is weak, the corresponding solution of Eq. (2.11) will also have a resonance at a nearby energy. The energy of the resonance or of the bound state of Eq. (2.12) would, in such a case, be a good approximation to the energy of the resonance obtained from an accurate solution of Eq. (2.11), i.e., to the resonance in the solution of the Schrödinger Eq. (2.3). The model resonance given by Eq. (2.12) may be shifted with respect to the actual resonance and it may have a different width. For narrow resonances, the size of the shift would be a good indication of the correctness of the model. The width of the actual resonance can typically be expected to be larger than the width of the model resonance as a result of the additional broadening due to the nonadiabatic coupling to other open states.

III. RESULTS

In this section, we analyze the dynamics of the lowest energy resonance in the F + XY → FX + Y reaction, where X and Y are H or D atoms, in terms of the model of the previous section, which is based on the adiabaticity of the XY vibration. We use the Muckerman V potential energy surface. Its parameters as well as the values of the physical constants used are the same as those of Ref. 18.[48,49]

The potential energy surface for the reaction is shown in Fig. 1 for each of the four isotopic systems FHD, FH_2, FD_2, and FDH. The corresponding skew angles are 37.3°, 46.4°, 47.7°, and 56.7°, respectively, and the effective masses μ, in units of the H atom mass, are 1.31, 0.95, 1.82, and 1.31, respectively. The differences among these angles and masses are ultimately responsible for the differences among the characteristic parameters of the resonances in these four systems.

The eigenvalues $\epsilon_\alpha^i(R_\alpha)$ of Eq. (2.7) for the potential $V(r_\alpha, R_\alpha)$ at fixed values of R_α were evaluated for each of the four isotopic systems as a function of the parameter R_α using the finite element method of Malik *et al.*[50] For the $F+H_2$ system, they are shown in Fig. 2 for a few values of R_α together with plots of $V(r_\alpha, R_\alpha)$ versus r_α. The variation of $\epsilon_\alpha^i(R_\alpha)$ with R_α for some i is shown in Fig. 3 for all four isotopic reactions. The eigenvalue $\epsilon_0^\alpha(R_\alpha)$, which correlates with the ground vibrational state of the unperturbed XY molecule at large R_α and is used to construct the adiabatic model for the resonance, is shown as a bold curve on that figure.

Equation (2.12) with $i=0$ was solved numerically using Gordon's method[51] to obtain the scattering phase shifts η at large R_α. The dependence of η on energy is shown in the upper part of Fig. 4 for the $F+H_2$ reaction. The rapid increase in η over a narrow energy range results in a sharp peak in the delay time $D=2\hbar(d\eta/dE)$ vs energy curve at the bottom of that figure. These features indidate the existence of a long-lived complex whose R_α motion is trapped by the $\epsilon_0^\alpha(R_\alpha)$ well of Fig. 3(b). The lower right ordinate scale in Fig. 4 gives the delay time in units of the fundamental vibration period of an R_α-motion harmonic oscillator whose zero-point energy is equal to the model resonance energy of the $\epsilon_0^\alpha(R_\alpha)$ well, indicated by the solid horizontal line in Fig. 3(b). The left lower ordinate scale of Fig. 4 is in units of an r_α-motion harmonic oscillator fundamental vibration period whose zero-point energy is equal to that of the $V(\bar{R}_\alpha, r_\alpha)$ potential, where $\bar{R}_\alpha$ is the value of R_α corresponding to the bottom of the $\epsilon_0^\alpha(R_\alpha)$ well. For the F + HD and $F+D_2$ systems, rapid increases of η with energy over a narrow energy range are also observed. The model resonance energies of the solutions of Eq. (2.12) are determined by the position of the maximum of the peak of the delay time vs energy curve analogous to Fig. 4 for each of the isotopic systems F + HD, $F+H_2$, and $F+D_2$.

The model resonance width for $F+H_2$ and $F+D_2$ are determined from the full width at half-maximum (FWHM) of the delay time vs energy curves. For the F + HD system, the thickness of the barrier in the effective potential $\epsilon_0(R_\alpha)$ at the model resonance energy of 0.237 eV is considerably larger than that at the exact resonance energy of 0.245 eV, and the FWHM of the delay time vs energy peak would furnish an artificially narrow width. A better estimate of the adiabatic part of this width can be obtained semiclassically. There are accurate uniform semiclassical formulas[52] for the width of the resonances of one-dimensional potentials such as that appearing in Eq. (2.12) in which the resonance energy enters as a parameter, and therefore, that width can be calculated at the exact resonance en-

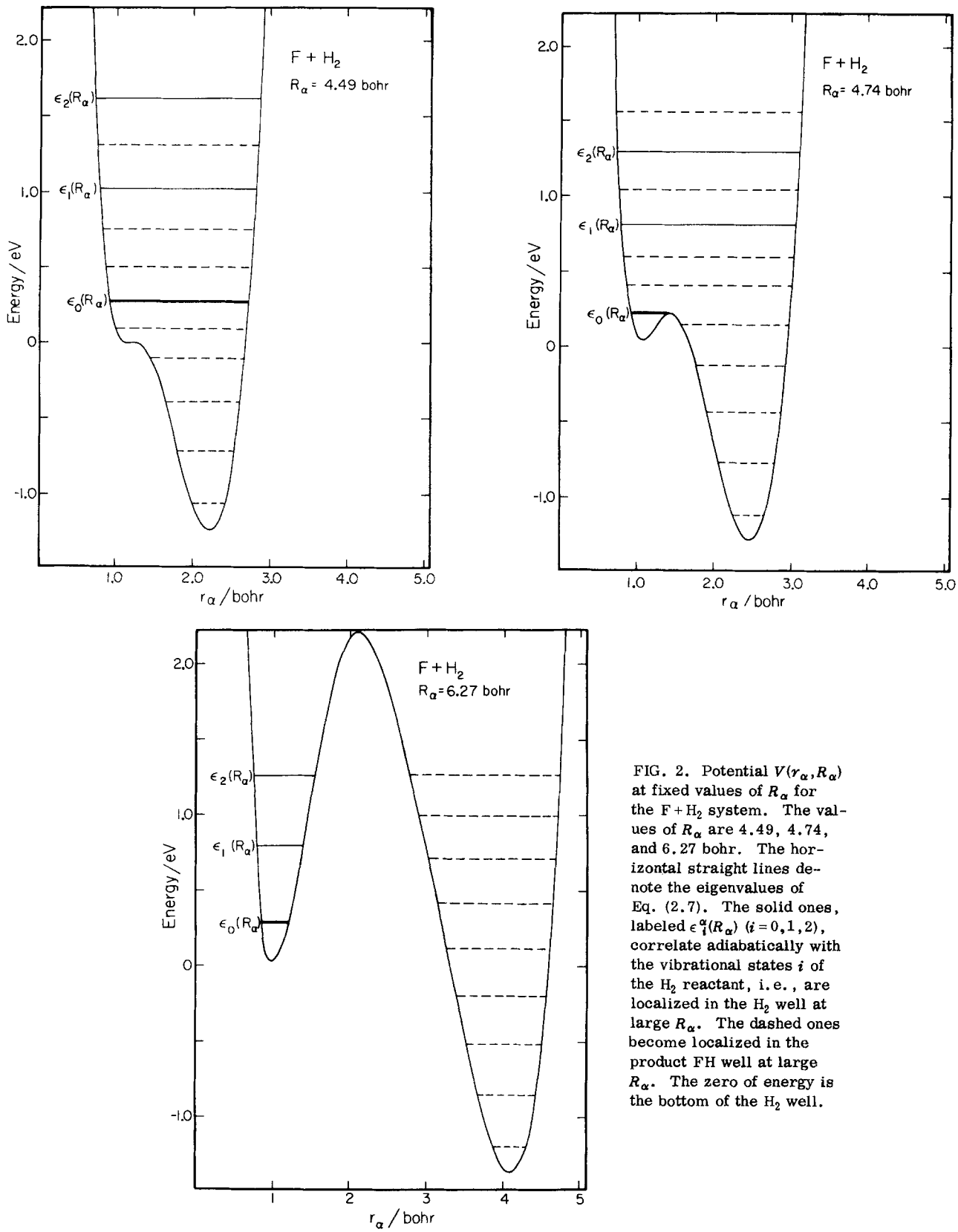

FIG. 2. Potential $V(r_\alpha, R_\alpha)$ at fixed values of R_α for the $F + H_2$ system. The values of R_α are 4.49, 4.74, and 6.27 bohr. The horizontal straight lines denote the eigenvalues of Eq. (2.7). The solid ones, labeled $\epsilon_i^\alpha(R_\alpha)$ $(i = 0,1,2)$, correlate adiabatically with the vibrational states i of the H_2 reactant, i.e., are localized in the H_2 well at large R_α. The dashed ones become localized in the product FH well at large R_α. The zero of energy is the bottom of the H_2 well.

ergy rather than at the model one. For the present purposes, one of the simplest semiclassical expressions is sufficiently accurate and is used. It is given by

$$\Gamma = \hbar \nu_0^\alpha \ln(1 + \epsilon^{-2Q^\alpha}) , \qquad (4.1)$$

where ν_0^α is the R_α vibrational frequency, taken here as the fundamental vibration frequency of an R_α motion harmonic oscillator whose zero-point energy is equal to the exact resonance energy measured with respect to the bottom of the $\epsilon_0(R_\alpha)$ well and Q^α is the tunneling phase

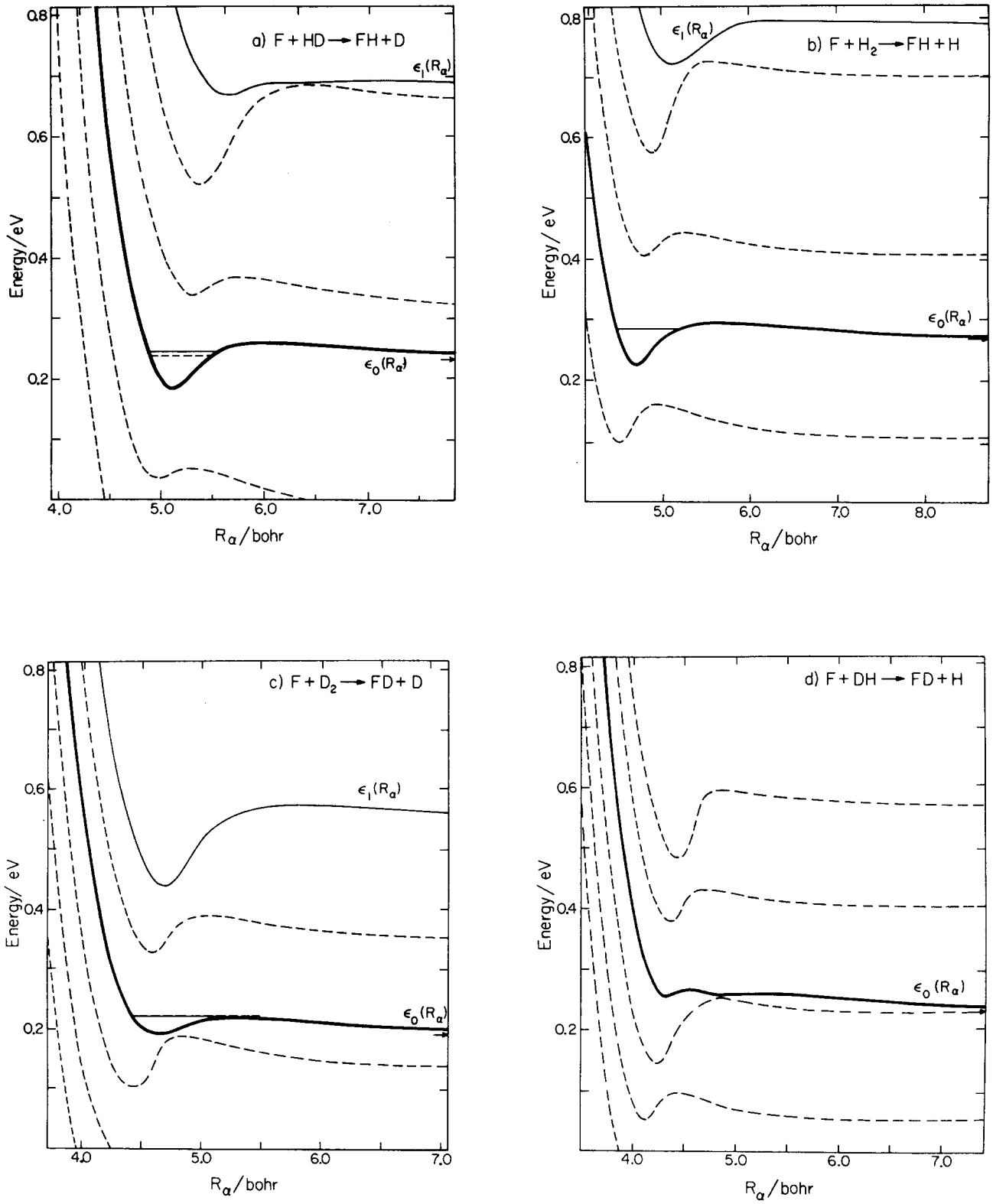

FIG. 3. The vibrational eigenvalues $\epsilon_i^{\alpha}(R_\alpha)$ of Eq. (2.7) as a function of R_α for all four isotopic variations. The zero of energy is the same as for Fig. 1. The $\epsilon_i^{\alpha}(R_\alpha)$ that correlate adiabatically to the XY vibrational eigenvalues at large R_α, i.e., which correspond to eigenfunctions that are localized in the reactant well at large R_α, are shown as full lines; the eigenvalues corresponding to eigenfunctions that are localized in the product well at large R_α are shown as dashed curves. The bold curve marked $\epsilon_0(R_\alpha)$, which correlates with the ground vibrational state of the reactants, is used in the adiabatic model of the lowest energy resonance. The horizontal line denotes the model resonance energy [Eq. (2.12)]. The horizontal dashed lines denote the exact resonance energy (E^P of Table I). The horizontal arrows ending at the right ordinate scale indicate the ground state energies of the isolated hydrogenic molecules. The length in mm, corresponding to 1 bohr in the abscissa of each of the four panels, has been scaled by the square root of the reduced mass of Eq. (2.3), i.e., in the ratio 1.14 : 0.97 : 1.35 : 1.14, for the FHD, FH_2, FD_2, and FDH R_α scales, respectively. With this scaling the R_α motion is associated with a particle of the same mass for all four systems.

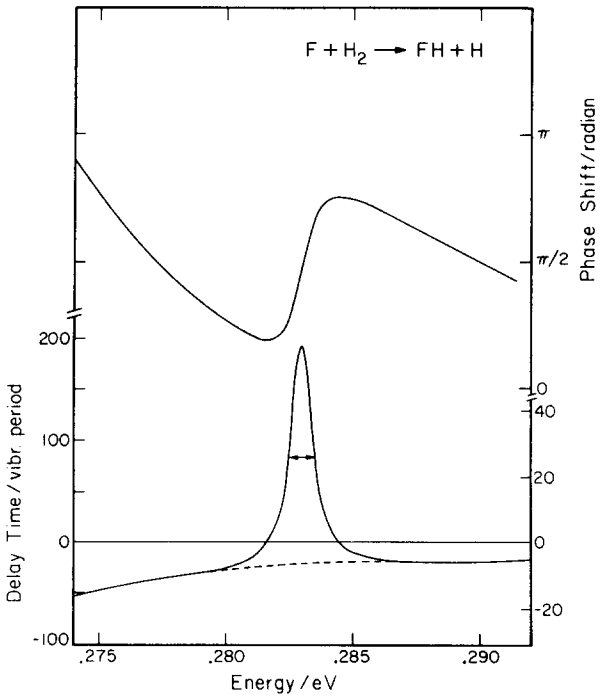

FIG. 4. Phase shifts and delay times obtained from the solution of Eq. (2.12) for the $F+H_2$ reaction. The effective potential $\epsilon_0^{\mathcal{J}}(R_\alpha)$ is shown in Fig. 3(b). The delay times are given in units of an R_α (lower left ordinate scale) and an r_α (lower right ordinate scale) vibrational period defined in the text.

integral given by

$$Q^\alpha = \int_{R_{\alpha<}}^{R_{\alpha>}} [\epsilon_0(R_\alpha) - E^{res}]^{1/2} dR \,, \qquad (4.2)$$

where E^{res} is the exact resonance energy and $R_{\alpha>}$ and $R_{\alpha<}$ are the two outermost turning points on the $\epsilon_0(R_\alpha)$ vs R_α at the energy E^{res}.

In Table I these model results are compared with the energies and the widths of the resonances obtained from the accurate coupled-channel calculations.[18,29] As seen from the table, an excellent agreement for the resonance energies is obtained for $F+H_2$, $F+HD$, and $F+D_2$. The differences between the exact resonance energies and the ones predicted by the model for $F+H_2$ and $F+D_2$ are actually smaller than the widths of the resonances, and such close agreement may be somewhat fortuitous. The resonance widths obtained from the present model reflect only the adiabatic contribution and may be viewed as an approximate lower bound to the actual resonance width.[53]

The accurate reaction probability vs energy curve for each of the four systems is given in Fig. 5.[18,29] It can be seen that the curve for the F + DH → FD + H system does not display a sharp structure analogous to that of the other three curves. However, a recent collision lifetime analysis[29] shows that a very short-lived (0.06 ps) lifetime does occur for this system at a total energy of 0.253 eV and an initial translational energy of 0.020 eV, significantly below the position of the probability peak at 0.044 eV translational energy. The present model does not predict this very weak resonant feature.

IV. DISCUSSION

The resonance positions and widths predicted by the present model agree reasonably well with those found in the accurate coupled-channel results for all but the very weak F + DH → FD + H resonance. Such agreement indicates that the model reproduces the essential dynamical features of the quasibound state which is responsible for the lowest energy resonances in the F + HD, $F+H_2$, and $F+D_2$ reactions. As a result, the model can be used to identify the important features of

TABLE I. Resonance energies and widths.

System	Resonant zero-point energy (meV)[a]	Resonance energy (meV)[b]			Resonance width (meV)	
		Present model	Exact Results E^{Pc}	Exact Results E^{qd}	Present model[e]	Exact results[f]
F+HD	232.9	237	244.9	244.9	0.28[g]	0.5
$F+H_2$	268.4	283	283.5	281.6	3	7.2
$F+D_2$	190.6	220	220.0	214.6	6	11.4
F+DH	232.9	...	h	253.3	...	21.2

[a]Zero-point energy of isolated hydrogenic molecule measured with respect to the bottom of that molecule's potential energy well.
[b]Total resonance energy, the zero of energy being the bottom of the isolated hydrogenic molecule well.
[c]Energy at which the accurate reaction probability of Fig. 5 has a maximum (Ref. 18).
[d]Energy at which the resonance eigenvalue of the collision lifetime matrix has a maximum (Ref. 29).
[e]The resonance widths given by the model reflect only the contribution of the adiabatic decay of the quasibound state into the ground state of the reactants.
[f]FWHM of the resonance collision lifetime matrix eigenvalue vs energy curve (Ref. 29).
[g]Obtained from a semiclassical expression associated with the tunneling through the barrier in the $\epsilon_0(R_\alpha)$ effective potential at the exact resonance energy of 0.2449 eV. See the text for details.
[h]The reaction probability vs energy curve for F+DH of Fig. 5 has a maximum at a total energy of 0.280 eV. However, comparison with the corresponding curves for the other three systems suggests that it is more likely to be due to a direct process occurring above the resonance energy than to the resonance referred to in footnote (c).

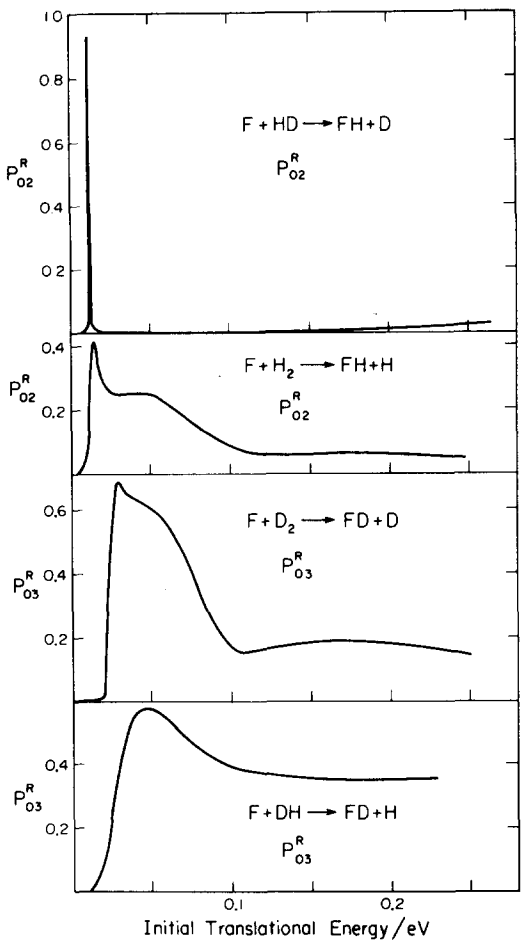

FIG. 5. Plot of the probability of the F + HD ($v = 0$) → FH($v' = 2$) + D, F + H_2 ($v = 0$) → FH ($v' = 2$) + H, F + D_2 ($v = 0$) → FD($v' = 3$) + D, and F + DH ($v = 0$) → FD ($v' = 3$) + H reactions (Refs. 18 and 29) as a function of the translational energy of the reactants.

these systems which lead to the existence, the energy, and the width of these resonances.

The quasibound states responsible for the resonances being considered are formed adiabatically from the separated F + XY reactants. As the F to XY distance decreases, the XY vibration, although somewhat distorted, retains its identity and quantum number, as well as its r_α direction of motion in the two-dimensional configuration space and becomes a distinct mode of motion of the complex. As a result, the effective potential $\epsilon_0(R_\alpha)$, which appears in Eq. (2.12), has a shape which depends largely on the shape of the potential energy function $V(R_\alpha, r_\alpha)$ along the R_α direction. In particular, the height of the barrier and the depth of the well in $\epsilon_0(R_\alpha)$, which play an important role in determining the characteristics of the resonance, correlate well with the features of $V(R_\alpha, r_\alpha)$ along R_α in the vicinity and to the left of the saddle point region. Very approximately, the values of $\epsilon_0(R_\alpha)$ are shifted upwards from those of $V(R_\alpha, r_\alpha)$ in the neighborhood of the minimum energy path, by the zero-point energy of the isolated XY hydrogenic molecule. This overall trend suggests that, in going from one isotopic system to another, the shift in the resonance energy should correlate approximately with the shift in the corresponding XY zero-point level. This is indeed the case, for both the model and the accurate results, as can be seen from a comparison of the second column of Table I with the next three. Thus, the qualitative nature of the variation of the position of the resonance with the isotopic system being considered is easily explained. A more quantitative explanation, encompassed in the model, includes the effects on the $\epsilon_0(R_\alpha)$ vs R_α curves of the changes produced in the r_α-motion zero-point energy by the approaching F atom.

The trend in the widths of the resonances, as we compare the several isotopic systems, is of a more subtle nature. Couplings of the entrance channel quasibound complex to both reagent and product states are involved, since both these couplings lead to its decay. The relatively narrow widths of those resonances for the FHD, FH_2, and FD_2 systems, as obtained from the coupled-channel calculations, indicates that the couplings of the multiplicative wave function described by Eq. (2.9) to other states is relatively weak. This weakness is, to some extent, due to the significant separation of the time scales of the motion along R_α and r_α in the complex, which separation in turn depends largely on the ratio of the effective masses for the motions along R'_α and r'_α being much larger than unity. This mass ratio M_α/m_α is about 4 for all four isotopic systems. Another factor is that the quasibound complex is in the ground vibrational state and its r_α motion is mainly confined to a strip of the potential energy surface along the $r_{\alpha_{\min}}(R_\alpha)$ path. In a considerable portion of the region of the surface in which the complex is localized, the potential energy function is separable within that strip, leading to the validity of Eq. (2.9) and consequently, to the weakness of the couplings of that state to other states which may lead to its decay.

Let us now analyze the nature of the couplings of the quasibound state to the reactant and product states. In the present systems, the decay of the resonance state into reactants occurs adiabatically into the ground vibrational state of the latter, and is due to tunneling through or motion over the effective dynamic potential barrier of the $\epsilon_0^a(R_\alpha)$ curve of Fig. 3 along the outward R_α direction. This R_α mode of motion of the complex transforms thereby into reactant translation, while the r_α mode remains largely unchanged and becomes the reactant vibration. The part of the resonance width that is due to this decay mechanism is controlled by the barrier traversal amplitude, i.e., by the likelihood of the system either tunneling through the barrier or moving over it, and is determined from the dependence of the phase shift resulting from Eq. (2.12) on energy for the F + H_2 and F + D_2 systems or from the tunneling coefficient at the exact resonance energy for the F + HD system. It is the only part of the width that can be readily estimated from the present model.

The complex can, in addition, decay into (or be formed from) the scattering states of the products. This decay pathway requires a more severe restructuring of the complex and involves vibrationally nonadiabatic processes. The enhancement of all of the state-to-state reactive transition probabilities in the reso-

nance energy region, seen in Fig. 5 and in the other exact reaction probability vs energy curves of Refs. 18 and 29, indicates that all the energetically accessible product states interact with the complex, although the present model furnishes an estimate of the strength of the interaction of the complex with the reactants, it does not lead to an estimation of its coupling with the products. The reason for this is that the coordinates that are appropriate for describing product states are different from those that are appropriate for describing the complex. The strength of the nonadiabatic coupling between two states is usually, to some extent at least, inversely proportional to the energy gap between them. One can therefore expect the energetically closest product state, in this case the highest accessible one, to interact the most strongly with the complex. An examination of the transition probabilities to different vibrational states of the product (Fig. 5 and Ref. 18) does indeed indicate the existence of such a trend.

The partial width of the resonance due to the coupling of the complex to the product states should roughly correspond to the difference between the exact width and the adiabatic partial width due to coupling with the reactants, determined in Sec. III, and presented in Table I. This difference, obtained from the last two columns of that table, suggests that the coupling to the product states is of the same order of magnitude as the coupling to the reactant states.

With these considerations in mind, let us attempt to interpret the trend in the resonance widths calculated for the FHD, FH_2, and FD_2 series by the model and by the coupled-channel method and displayed in the last two columns of Table I. A noticeable feature in that series is the broadening of the resonances in the order given. The potential energy surface for all three systems is the same function of the internuclear coordinates. However, when expressed in the (unscaled) Jacobi Cartesian coordinates R'_α, r'_α, some differences appear. The surfaces for FH_2 and FD_2 continue to be equal to each other in these coordinates, but that for FHD is slightly different, due to the shift of the center of mass of HD away from its midpoint and to the change of the (unscaled coordinate) skew angle from $\tan^{-1}2 = 63.4°$ to $\tan^{-1}3 = 71.6°$. In the following qualitative discussion, this small difference will be disregarded. In addition, although the mass m_α changes from $\frac{1}{2}$ to $\frac{2}{3}$ atomic hydrogen mass units in going from F + H_2 to F + HD, the effect of this change on the ϵ_0 vs R'_α (rather than R_α) curve is also small. The reason for this smallness is that $\epsilon_0(R'_\alpha)$ depends largely on the characteristics of $V(R'_\alpha, r'_\alpha)$ in the general vicinity of its saddle point, and only to a minor extent on m_α, as is also the case for $\epsilon_0(R_\alpha)$. As a result, $\epsilon_0(R'_\alpha)$ is approximately the same for those two systems. The most important difference between them is due to M_α, which is 1.81 and 2.59 atomic hydrogen mass units for F + H_2 and F + HD, respectively. The effect of this mass change is to lower the energy of the quasibound state in Eq. (2.12) [with respect to the bottom of the $\epsilon_0(R'_\alpha)$ well] by approximately the square root of the ratio of these masses. An equivalent way of arriving at the same conclusion is to replace the variable R_α in that equation by the variable $\rho_\alpha = \mu^{1/2}R_\alpha = M_\alpha^{1/2}R'_\alpha$ (as done in Fig. 3). This makes the well in the $\epsilon_0(\rho_\alpha)$ vs ρ_α curve for F + HD be somewhat broader than for the F + H_2 one, but the new effective mass in the transformed equation is now the same for both systems, resulting in the lowering of the quasibound level. This lowering results in the increase of the thickness of the barrier through which tunneling must occur for the system to move from this well region to the reactant region. Since the lifetime associated with the tunneling increases exponentially with this thickness, the resonance lifetime for FHD is larger than that of FH_2. In going from FHD to FD_2, the $\epsilon_0(\rho_\alpha)$ well width increases further, which would tend to make the lifetime of the FD_2 resonance longer than that of the FHD one. However, as can be seen from Fig. 3(c), an avoided crossing between the $\epsilon_0(R_\alpha)$ curve and another one [which localizes the corresponding eigenfunction $\phi_i(r_\alpha; R_\alpha)$ in the product region] reduces the depth of the well in this curve and pushes the corresponding quasibound state slightly higher than the top of the barrier. This effect is dominant and results in an FD_2 resonance broader than those for the FHD and FH_2 systems. It should be noted that this analysis refers to the adiabatic part of the resonance width. The nonadiabatic part associated with the interaction of the complex with the products should further depend on the Delves coordinate skew angle, and should increase as this angle increases, in the direction FHD, FH_2, FD_2 as is observed in the accurate calculations.

Another consequence of the analysis above is that the resonance characteristics are very sensitive to the shape and size of the barrier in the effective potential $\epsilon_0(R_\alpha)$ vs R_α curve and therefore, on the shape and size of the barrier in the $V(R_\alpha, r_\alpha)$ surface along the R_α direction. As a result, small changes in the details of the saddle point region of the surface (smaller in magnitude than 1 kcal/mole) can be expected to introduce radical changes in the resonance characteristics, including the possibility of their complete disappearance. Consequently, such resonances will constitute a very sensitive probe for the experimental characterization of that region of the FH_2 potential energy surface.

As observed in Fig. 5, the off-resonance transition probabilities for the F + H_2 and F + D_2 reactions are much larger than for the F + HD one. This behavior can be understood by considering that the pronounced narrowness of the FHD resonance is a manifestation of the weakness of the coupling of the reactant states to the product states through the strong interaction (complex) region, with a resulting small reaction probability away from resonance when compared with the other two systems.

The present model for the resonance in the F + H_2, F + HD, and F + D_2 reactions is similar to the one used by Chapman and Hayes,[35,41] to study the resonances in I + H_2 reactive collisions and in He^* + H_2 inelastic collisions. In their model, a zero-order approximation for the wave function of the complex is obtained in the form $\psi = \bar{g}(R'_\alpha)\bar{\phi}(r'_\alpha)$, where $\bar{\phi}(r'_\alpha)$ is the isolated reagent diatomic molecule wave function and $\bar{g}(R'_\alpha)$ is the eigenfunction associated with $V(R'_\alpha; r'_{\alpha_{eq}})$, i.e., calculated

along the potential energy surface with r'_α fixed at its isolated reagent equilibrium position. The distortion of the diatomic molecule during the collision is accounted for by a first-order perturbation correction to the asymptotic eigenvalues. The nature of the resonances in the present systems is, however, markedly different from the ones in $He + H_2^+$ and $I + H_2$. The latter are supported by actual two-dimensional potential energy wells in the corresponding surfaces. No such wells exist in the present case, and the origin of the stability of the complex is of a purely dynamical nature.

The quantum dynamics of the resonances in one of the reactions studied here, namely $F + H_2$, has been a subject of a detailed study by Latham *et al.*[20] by means of a vibrationally adiabatic analysis, a vibrational entropy analysis, and a scattering wave function probability density analysis. Their vibrationally adiabatic analysis in a system of curved reaction coordinates shows that no single channel model in those coordinates can account for the resonances, whereas in our model it does. The sharp increase in the scattering wave function probability density in a small region of the surface at the resonance energy indicates clearly the location on the surface where the complex is formed. The location of the complex predicted by the present model appears to be in reasonable agreement with that indicated by the scattering probability density maps in Ref. 20.

Another study of the resonances on the $F + H_2$ reaction by Hayes and Walker[54] came to our attention during the preparation of this manuscript. One of the aspects of their work is the study of the sensitivity of the resonances to the shape of the potential in the entrance channel. They have shown that if the entrance channel barrier is removed from the surface, the scattering results on the new surface do not show a resonance. The disappearance of the resonance as a result of this removal is in agreement with the conclusions drawn above from the validity of the present model.

Although the present study was done using only one semiempirical surface, most of the collinear $F + H_2$ surfaces used so far[18-23] have similar basic features, and we hope that our model will also be useful for predicting the absence or presence and the characteristics of this type of resonance on other more accurate surfaces for the $F + H_2$ reaction.

Resonances of a similar nature can be expected to be seen in other exothermic reactions with a small barrier early in the entrance channel. The present type of analysis can also be expected to be useful in modeling resonances in low barrier asymmetric reactions of the heavy–light–heavy type. On the other hand, this approach will be less useful for reactions with light–heavy–light (LHL) mass combinations since the reagent vibrational motion is in such cases almost parallel to the the product translational motion (in configuration space) making it unlikely that a complex of the present type would exist. In the limit of infinite central atom mass, even Eq. (2.11) becomes invalid. The resonances in thermoneutral or nearly thermoneutral reactions of the LHL type usually have a different physical origin and can be successfully modeled using different techniques.[38]

Removing the collinear restriction from the motion of the triatomic complex would introduce changes in its dynamics which are, as shown previously for the case of the $H + H_2$[30] and $F + H_2$[24] systems, to a certain extent, predictable. The equilibrium configuration of the complex would, based on the structure of the surface, remain collinear. There would be two additional degrees of freedom of the complex, described either as a doubly degenerate hindered rotation or a doubly degenerate bending vibration. For the resonances studied here, they are likely to be most separable if treated as hindered rotations of the H_2 molecule around its center of mass. The existence of these two additional modes of motion would shift the energy of the complex for collisions with zero total angular momentum upwards by the sum of their zero-point energies.[30]

The most serious complication introduced by removing the collinear restriction for the $F + H_2$ reaction is the large number of possible rotational states of the complex that spread over a wide energy range. As a result, the long-lived complex can be formed, as shown by approximate coupled-channel calculations,[24] over a wide range of collisional energies and does not produce strong structure in the integral reaction cross section vs energy curve. However, angular distributions of reaction products are expected to be quite different at resonance energies as compared with the nonresonance ones.[24,25,27,28,30] As a result, it is important to develop models that predict the shape of the differential reaction cross section vs scattering angle curves at resonance. Such models could permit the establishment of relations between the characteristics of the shape of the potential energy surface in the strong interaction region and characteristics of those angular distributions. These relationships would be very useful in extracting information about the details of potential energy surfaces from experimental observations of reactive scattering resonances.

V. SUMMARY

The results and conclusions given in the present paper can be summarized as follows:

(1) The lowest resonance in the collinear reactions $F + H_2(v=0) \rightarrow FH + H$, $F + HD(v=0) \rightarrow FH + D$, and $F + D_2(v=0) \rightarrow FD + D$ is due to the formation of a quasibound complex which is localized in the entrance channel region of the corresponding potential energy surface, slightly to the left of its saddle point.

(2) The ordering of the positions of these resonances is the same as that of the zero-point energies of the reactant molecules. The reason for this interrelation is that the shape of the effective potential in the R_α direction, which correlates adiabatically with the ground state of the reactant, is determined largely by the shape of the potential energy surface $V(R_\alpha, r_\alpha)$ along R_α.

(3) The nonadiabatic coupling of the complex to the reaction products is of the same order of magnitude as its adiabatic coupling to the reagents.

(4) The adiabatic part of the resonance width increases in the order FHD, FH_2, FD_2. The increase from

FHD to FH_2 is due to a corresponding lowering of the effective adiabatic barrier height. The increase from FH_2 to FD_2 is due to a decrease of the depth of the adiabatic well.

(5) The position and width of the resonance is a very sensitive function of the shape of $V(R_\alpha, r_\alpha)$ in the saddle point region and may change or the resonances may even disappear if that region of the potential is modified.

ACKNOWLEDGMENTS

This work was supported in part by a grant from the National Science Foundation (No. CHE77-26515). The research reported made use of the Dreyfus–NSF Theoretical Chemistry Computer which was funded through grants from the Camille and Henry Dreyfus Foundation, the National Science Foundation (Grant No. CHE78-20235), and the Sloan Fund of the California Institute of Technology. We would like to thank Mr. Jack A. Kaye for help with the coupled-channel calculations, and Dr. E. F. Hayes for useful discussions.

[1]J. C. Polanyi and J. L. Schreiber, Faraday Discuss. Chem. Soc. **62**, 267 (1977) and the discussion therein.
[2]J. B. Anderson, Adv. Chem. Phys. **41**, 229 (1980).
[3]C. F. Bender, S. V. O'Neil, P. K. Pearson, and H. F. Schaefer, Science **176**, 1912 (1972); C. F. Bender, P. K. Pearson, S. V. O'Neil, and H. F. Schaefer, J. Chem. Phys. **56**, 4626 (1972); C. F. Bender and H. F. Schaefer, in *Fluorine Containing Free Radicals*, ACS Symposium Series, edited by J. W. Roth (American Chemical, Wash., D.C., 1978), p. 283; S. R. H. F. Schaefer and B. Liu, Faraday Discuss. Chem. Soc. **62**, 330 (1977).
[4]R. L. Jaffe, K. Morokuma, and T. F. George, J. Chem. Phys. **63**, 3417 (1975).
[5]F. Rebentrost and W. A. Lester, Jr., J. Chem. Phys. **63**, 3737 (1975).
[6]B. Liu, J. Chem. Phys. **58**, 1925 (1973); P. Siegbahn and B. Liu, *ibid.* **68**, 2457 (1978).
[7]D. G. Truhlar and C. G. Horowitz, J. Chem. Phys. **68**, 2466 (1978).
[8]J. B. Anderson, J. Chem. Phys. **52**, 3849 (1970).
[9]N. Jonathan, S. Okuda, and D. Timlin, Mol. Phys. **24**, 1143 (1972).
[10]J. T. Muckerman, J. Chem. Phys. **54**, 1155 (1971); **56**, 2997 (1972); **57**, 3388 (1972).
[11]J. C. Polanyi and J. L. Schreiber, Chem. Phys. Lett. **29**, 319 (1974).
[12]R. L. Wilkins, J. Chem. Phys. **57**, 912 (1972); **58**, 3038 (1973); J. Phys. Chem. **77**, 3081 (1973).
[13]D. L. Thompson, J. Chem. Phys. **57**, 4170 (1972).
[14]N. C. Blais and D. G. Truhlar, J. Chem. Phys. **58**, 1090 (1973).
[15]A. M. G. Ding, L. J. Kirsch, D. S. Perry, J. C. Polanyi, and J. L. Schreiber, Faraday Discuss. Chem. Soc. **55**, 252 (1973).
[16]R. L. Jaffe, K. Morokuma, and T. F. George, J. Chem. Phys. **63**, 3417 (1975).
[17]D. Feng, E. R. Grant, and J. W. Root, J. Chem. Phys. **64**, 3450 (1976).
[18](a) G. C. Schatz, J. M. Bowman, and A. Kuppermann, J. Chem. Phys. **58**, 4023 (1973); (b) **63**, 674 (1975); (c) **63**, 685 (1975).
[19]S. F. Wu, B. R. Johnson, and R. D. Levine, Mol. Phys. **25**, 839 (1973).
[20]S. L. Latham, J. F. McNutt, R. E. Wyatt, and J. J. Redmon, J. Chem. Phys. **69**, 3746 (1978).
[21]J. N. L. Connor, W. Jakubetz, and J. Manz, Mol. Phys. **29**, 347 (1975); **35**, 1301 (1978); **39**, 799 (1980).
[22]J. T. Adams, R. L. Smith, and E. F. Hayes, J. Chem. Phys. **61**, 2193 (1974).
[23]J. C. Light and R. B. Walker, J. Chem. Phys. **65**, 4272 (1976).
[24]M. J. Redmon and R. E. Wyatt, Chem. Phys. Lett. **63**, 209 (1979).
[25]Y. Shan, B. H. Choi, R. T. Poe, and K. T. Tang, Chem. Phys. Lett. **57**, 379 (1978).
[26]T. P. Schafer, P. E. Siska, J. M. Parson, E. P. Tully, Y. C. Wong, and Y. T. Lee, J. Chem. Phys. **53**, 3385 (1970); Y. T. Lee, in *Physics of Electronic and Atomic Collisions*, edited by T. R. Grovers and F. J. deHeer (North–Holland, Amsterdam, 1971), p. 357.
[27]R. K. Sparks, C. C. Hayden, K. Shobatake, D. M. Neumark, and Y. T. Lee, in *Horizons of Quantum Chemistry: Proceedings of the Third International Congress of Quantum Chemistry*, edited by K. Fukui and B. Pullman (Reidel, Boston, 1980), pp. 91–105.
[28]A. Kuppermann, in *Potential Energy Surfaces and Dynamics Calculations*, edited by D. G. Truhlar, (Plenum, New York, 1981), pp. 375–420.
[29]A. Kuppermann and J. A. Kaye, J. Phys. Chem. **85**, 1969 (1981).
[30]G. C. Schatz and A. Kuppermann, Phys. Rev. Lett. **35**, 1266 (1975); J. Chem. Phys. **65**, 4668 (1976).
[31]W. D. Miller, S. A. Safron, and D. R. Herschbach, Faraday Discuss. Chem. Soc. **44**, 108 (1967); J. M. Blatt and V. F. Weisskopf, *Theoretical Nuclear Physics* (Wiley, New York, 1952), pp. 532–542.
[32]D. Secrest and W. Eastes, J. Chem. Phys. **56**, 2502 (1972); **58**, 1271 (1973).
[33]W. Eastes and R. A. Marcus, J. Chem. Phys. **59**, 4757 (1973).
[34]E. J. Shipsey, J. Chem. Phys. **56**, 1179 (1972).
[35]F. M. Chapman, Jr. and E. F. Hayes, J. Chem. Phys. **62**, 4400 (1975); **65**, 1032 (1976).
[36]R. D. Levine and S. F. Wu, Chem. Phys. Lett. **11**, 557 (1971).
[37]A. Kuppermann and J. P. Dwyer, in *Electronic and Atomic Collisions* [Abstracts of Contributed Papers, XIth International Conference on the Physics of Atomic Collisions], edited by K. Takayanagi and N. Oda (The Society for Atomic Collision Research, Japan, 1979), pp. 888–889; J. P. Dwyer, Ph. D. Thesis, California Institute of Technology (1977).
[38]V. K. Babamov and A. Kuppermann (manuscript in preparation).
[39]D. W. Noid and M. L. Kozzykowski, Chem. Phys. Lett. **73**, 114 (1980); M. L. Koszykowski, Ph. D. thesis, University of Illinois at Urbana–Champaign (1978); D. W. Noid, M. L. Koszykowski, and R. A. Marcus, in *Classical, Semiclassical, and Quantum Mechanical Problems in Mathematics, Chemistry and Physics*, edited by K. E. Gustavson and W. P. Reinhardt (Plenum, New York, 1981), p. 133.
[40]J. R. Stine and R. A. Marcus, Chem. Phys. Lett. **29**, 575 (1974); J. R. Stine, Ph. D. thesis, University of Illinois at Urbana–Champaign (1975).
[41]F. M. Chapman, Jr. and E. F. Hayes, J. Chem. Phys. **66**, 2554 (1977).
[42]L. M. Delves, Nucl. Phys. **9**, 391 (1959); *ibid.* **20**, 275 (1960).
[43]B. I. Stepanov, Nature **157**, 808 (1946); Zh. Fiz. Khim. **19**, 507 (1945); **20**, 907 (1946); N. D. Sokolov and V. A. Savel'ev, Chem. Phys. **22**, 383 (1977); S. A. Barton and W. R. Thorson, J. Chem. Phys. **71**, 4263 (1979).
[44]M. Born and R. Oppenheimer, Ann. Phys. (Leipzig) **84**, 57 (1927); M. Born and K. Huang, *Dynamical Theory of Crystal Lattices* (Oxford University, Oxford, England, 1954).
[45]V. K. Babamov and R. A. Marcus, J. Chem. Phys. **74**, 1790 (1981).

[46]J. A. Kaye and A. Kuppermann, Chem. Phys. Lett. **77**, 573 (1981).
[47]See, for example, V. K. Babamov, J. Chem. Phys. **69**, 3414 (1978).
[48]The value of the equilibrium H_2 distance used for the calculations reported in Ref. 18 was $r=1.7419$ Å. It is misprinted in Ref. 18 as $r=1.7149$ Å. The masses of the H, D, and F atoms used are 1836.95, 3675.43, and 34692.20 a.u., respectively.
[49]There are small differences in the resonance energies found in different coupled-channel calculations on the Mukcerman V potential energy surface in the literature due to slight variations in the equilibrium parameters and physical constants used as well as to the use of different analytic fits to the surface.
[50]D. J. Malik, J. Eccles, and D. Secrest, J. Comput. Phys. **38**, 157 (1980).
[51]R. G. Gordon, J. Chem. Phys. **51**, 14 (1969); Methods Comput. Phys. **10**, 81 (1979).
[52]J. N. L. Connor and D. Smith, Mol. Phys. **43**, 397 (1981), and references cited therein.
[53]However, when the resonance energy found by the model is significantly higher than the exact one (which is not the present case), the width of the model resonance can be larger than that of the exact results due to a possible overestimate of the likelihood of adiabatic decay.
[54]E. F. Hayes and R. B. Walker, J. Phys. Chem. **86**, 85 (1982).